Supporting Information

Ru-Porphyrin metal-organic frameworks with Mn2 paddlewheel nodes for C(sp^3)-H bonds selective oxidation

Contents

1. Experimental Section.

Materials and Methods

Manganese (II) chloride tetrahydrate ($MnCl_2 \cdot 4H_2O$), triruthenium dodecacarbonyl ($C_{12}O_{12}Ru_3$), methyl p-formyl benzoate, N, N-Dimethylformamide (DMF) and hydrochloric acid were purchased from Energy Chemical. Tert-butyl hydroperoxide solution (TBHP) was purchased from Shanghai Macklin Biochemical Co., Ltd. All substrates were purchased from Aladdin. Pyrrole and all the solvent were purchased from Tianjin Kemiou Chemical Reagent Co., Ltd.

All the chemicals were of analytical grade and used as received without any purification. Oxidation and nitrogen (99.995%) were purchased from Dalian Institute of Special Gases and used as received. Powder XRD diffractograms were obtained on a Rigaku D/Max-2400 X-ray diffractometer with a sealed Cu tube (λ = 1.54178 Å). in the angular range 2θ = 5-50° at 293 K. ^{1}H NMR data were collected on a Varian INOV A-600 MHz, Bruker Advance III 400 MHz spectrometer at ambient temperature. Fourier transform infrared (FT-IR) spectra were recorded as KBr pellets on JASCO FT/IR-430 spectrometer. Thermogravimetric analyses (TGA) were carried out at a ramp rate of 10 °C min^{-1} in nitrogen flow with a SDTQ600 instrument. Electron paramagnetic resonance (EPR) experiments were conducted on a Bruker E500 instrument, and the intensity was recorded at 298 K. X-ray photoelectron spectroscopy (XPS) signals were collected on a Thermo ESCALAB Xi+ spectrometer. The light source was a 450 nm LED, which was purchased from Beijing China Education Au-

light Co., Ltd.

Gas Adsorption Studies.

All nitrogen adsorptions experiments were measured on a Quanta chrome Autosorb-1 automatic volumetric instrument. The N_2 adsorption isotherms for desolated compounds were collected in a relative pressure range from 10 to 1.0×10^5 Pa. A liquid nitrogen bath (77 K) was used for isotherm measurements. Ultra-high purity grade N_2 was used to the adsorption experiments.

1.1 Substrate encapsulation experiments

The substrate-impregnated crystals were obtained by soaking crystals of Mn−TCPP(Ru) in a solution of the substrate in acetonitrile (1.0 M) for 48 h. After the soaked crystals was washed with acetonitrile, the substrate-loaded crystals were confirmed by using IR spectroscopy.

1.2 EPR detection of superoxide radical

The production of the short-lived radical $^{\bullet}OO^{t}Bu$ by Mn−TCPP(Ru) in the presence of n-tert-butyl-α-phenylnitrone (PBN) was detected by EPR. Typically, 0.5 mol/L PBN in 1 mL CH_3CN was mixed with 0.5 mL Mn−TCPP(Ru)/CH_3CN suspension (0.5 mg/mL). The resulting mixture (400 μL) was added to the EPR tube.

Preparation

Scheme S1. Synthesis procedure of ligand TCPP(Ru)

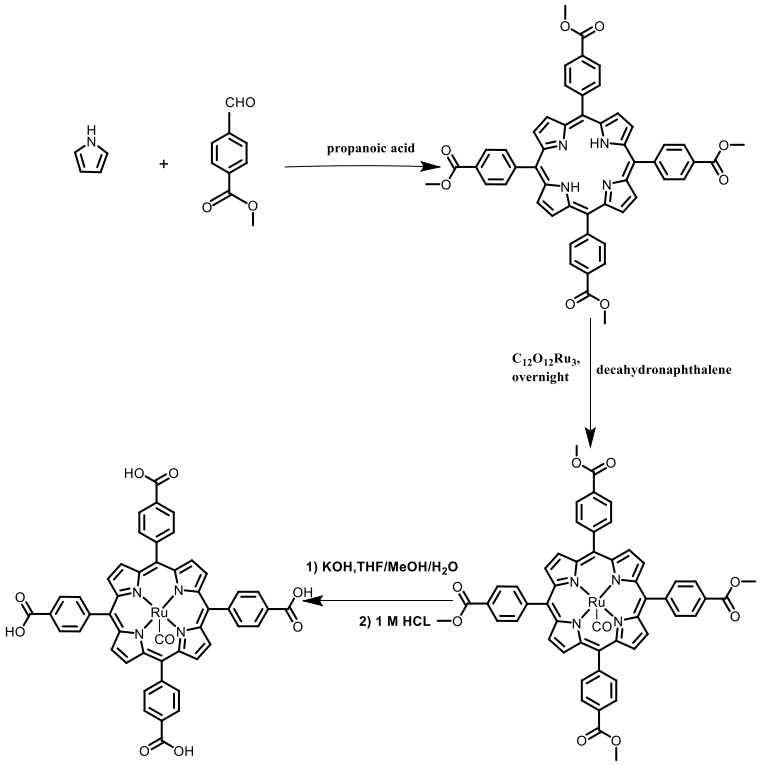

(1) Synthesis of compound TPPCOOMe

The procedure referenced existing literature. [S1] A solution of methyl p-formyl benzoate (6.9 g, 42.0 mmol) in 100 mL of propionic acid was stirred until completely dissolved. Pyrrole (3 mL, 43.0 mmol) was added dropwise to the solution through a constant pressure dropping funnel. The mixture was then stirred at reflux at 150 °C for 12 hours. After cooling to room temperature, the precipitate was collected by filtration and washed sequentially with methanol, ethyl acetate and tetrahydrofuran. The purple solid was dried under vacuum and collected. Yield: 1.86 g, 21%. ^{1}H NMR (400 MHz, $CDCl_3$): δ 8.80 (s, 8H), 8.43 (d, J = 8 Hz, 8H), 8.28 (d, J = 8 Hz, 8H), 4.11 (s, 12H), −2.83 (s, 2H).

(2) Synthesis of porphyrin complex TPPCOOMe(Ru)

The procedure referenced existing literature.[2] TPPCOOMe (500 mg, 0.59 mmol) and $Ru_3(CO)_{12}$ (450 mg,0.70 mmol) were refluxed in decalin (150 mL) for 24 h, and then the reaction mixture was allowed to cool down to room temperature. The resulting solid was separated from the solvent by vacuum filtration and purified by column chromatography with ethyl acetate/methylene chloride (1:100 v/v). The bright red band was collected and evaporated to dryness to obtain the desired product. Yield: 91%. ^{1}H NMR (400 MHz, $CDCl_3$) δ 8.63 (m, 8 H), 8.40 (m, 8 H), 8.26 (m, 8 H), 4.09 (s, 12 H).

(3) Synthesis of TCPP(Ru)

The procedure referenced existing literature. [S2] TPPCOOMe (Ru) (1.0 g, 1.1 mmol) was stirred in a mixture of THF (25 mL) and MeOH (25 mL). To this solution was added a solution of KOH (2.7 g, 47.2 mmol) in H_2O (25 mL). The mixture was refluxed for 24 hours. After refluxing, THF and MeOH were removed by rotary evaporation under reduced pressure. Additional water was added to the solution and the solution was acidified with 1 M HCl until no further precipitation occurred. The solid was collected by filtration, washed with water and then dried in vacuum to give a bright red solid. Yield: 93%. ^{1}H NMR (400 MHz, DMSO-d_6) δ 8.58 (s, 8 H), 8.34 (m, 12 H), 8.20 (m, 4 H).

(4) Preparation of Mn−TCPP(Ru)

A mixture of TCPP(Ru) (10.0 mg, 12 μmol), $MnCl_2$-$4H_2O$ (20.0 mg, 0.1 mmol), and hydrochloric acid (100 μL) was dissolved in 2 mL of DMF solvent, and the solution was placed in a screw cap vial. The resulting mixture was kept in an oven at 140°C for 48 hours. After the autoclave was cooled to room temperature, it was washed with DMF,

H_2O and ethanol, centrifuged for a long time and air-dried to obtain purple single crystals. Yield: 61%. Anal. Calcd. For $C_{50}H_{24}Mn_2N_4O_{13.5}Ru$. IR (KBr): 3354 (br), 1940(s), 1594(dt), 1405(vs), 1097(s), 1008(s), 776(m) cm^{-1}.

2. Single Crystal X-ray Crystallography

The intensities were collected on a Bruker SMART APEX CCD diffractometer equipped with a graphite-monochromated Mo Kα (λ = 0.71073 Å) radiation source; the data were acquired using the SMART and SAINT programs. The structure was solved by direct methods and refined by full matrix least-squares methods by the program SHELXL-2014.[S3]

In the structural refinement of Mn−TCPP(Ru), all of the non-hydrogen atoms were refined anisotropic ally. The hydrogen atoms within the ligand backbones were fixed geometrically at calculated distances and allowed to ride on the parent non-hydrogen atoms. To assist the stability of refinements, the thermal parameters on adjacent atoms in vanadium-porphyrin were restrained to be similar. The SQUEEZE subroutine in PLATON was used. [S4]

Table S1. Crystal data and structure refinements.

Compound	Mn−TCPP(Ru)
Empirical formula	$C_{73}H_{86}ClMn_2N_{12}O_{19}Ru$
Formula weight	1681.93
Temperature/K	120.15
Crystal system	monoclinic
Space group	I2/m
a/Å	9.951(3)
b/Å	23.683(5)
c/Å	19.487(5)
α/°	90
β/°	101.800(14)
γ/°	90
Volume/Å^3	4495(2)
Z	2
ρ_{calc}g/cm^3	1.243
μ/mm^{-1}	0.538
F (000)	1742.0
Crystal size/mm^3	0.2 × 0.18 × 0.16
Radiation	MoKα (λ = 0.71073)
2Θ range for data collection/°	4.522 to 50.046
Index ranges	$-11 \le h \le 11$, $-28 \le k \le 28$, $-23 \le l \le 23$
Reflections collected	65738
Independent reflections	4066 [R_{int} = 0.0833, R_{sigma} = 0.0312]
Data/restraints/parameters	4066/18/188
Goodness-of-fit on F^2	1.046
Final R indexes [I>=2σ (I)]	R_1 = 0.0538, wR_2 = 0.1533
Final R indexes [all data]	R_1 = 0.0656, wR_2 = 0.1644
Largest diff. peak/hole / e Å^{-3}	1.80/-0.48
CCDC number	2329349

Table S2. Selected bond lengths (Å) for Mn−TCPP(Ru).

Bond	Bond Length/Å
Ru1-N1	2.054(3)
Ru1-N11	2.054(3)
Ru1-N12	2.054(3)
Ru1-N13	2.054(3)
Ru1-C11	1.970(6)
Ru1-C112	1.970(6)
Ru1-O2	1.970(6)
Mn1-Mn14	3.1751(18)
Mn1-O5	2.276(17)
Mn1-O34	2.116(4)
Mn1-O15	2.106(3)
Mn1-O16	2.106(3)
Mn1-O4	2.114(4)

3. Characterizations of Metal−Organic Framework Mn−TCPP(Ru).

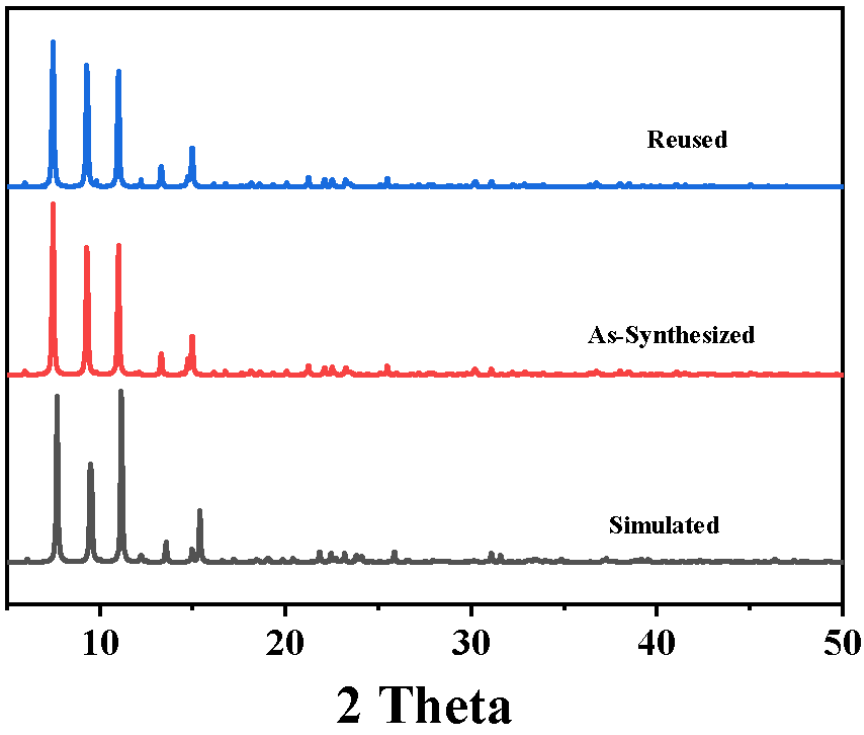

Figure S1. PXRD patterns of Mn−TCPP(Ru) (red), its calculated pattern based on the single-crystal (black) and PXRD patterns of Mn−TCPP(Ru) after 5-time catalysis

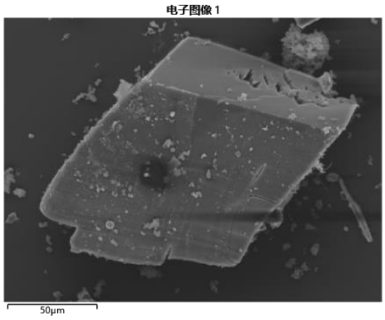

Figure S2. SEM image for fresh Mn−TCPP(Ru).

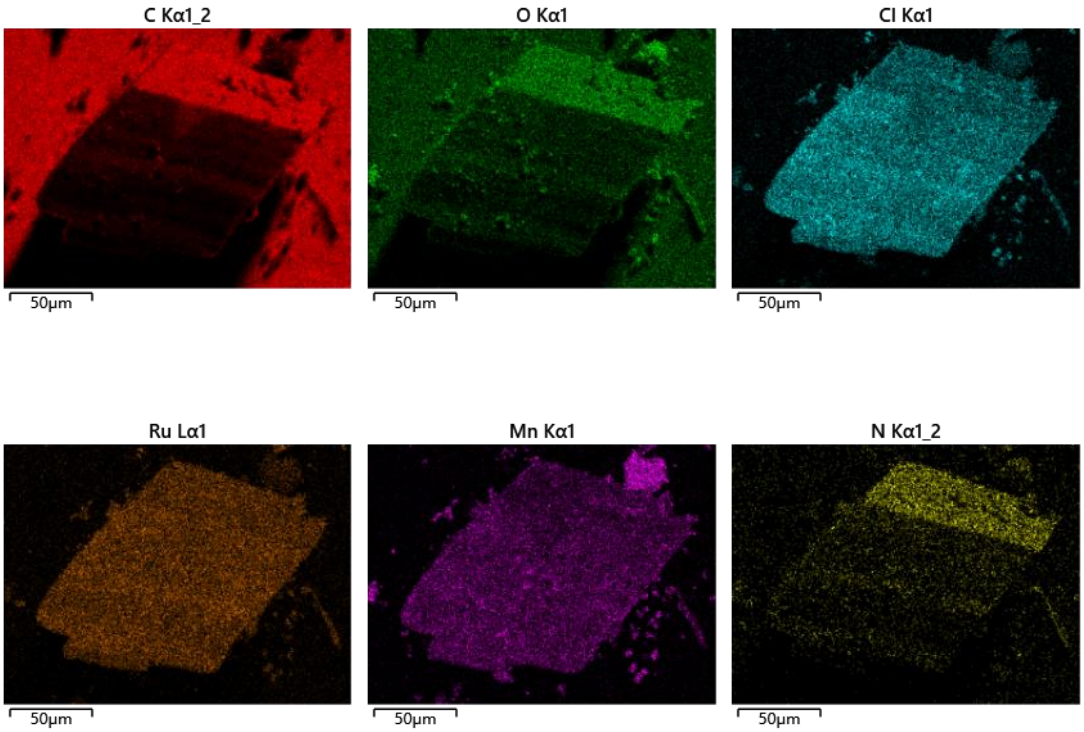

Figure S3. SEM image and corresponding EDS maps for fresh Mn−TCPP(Ru).

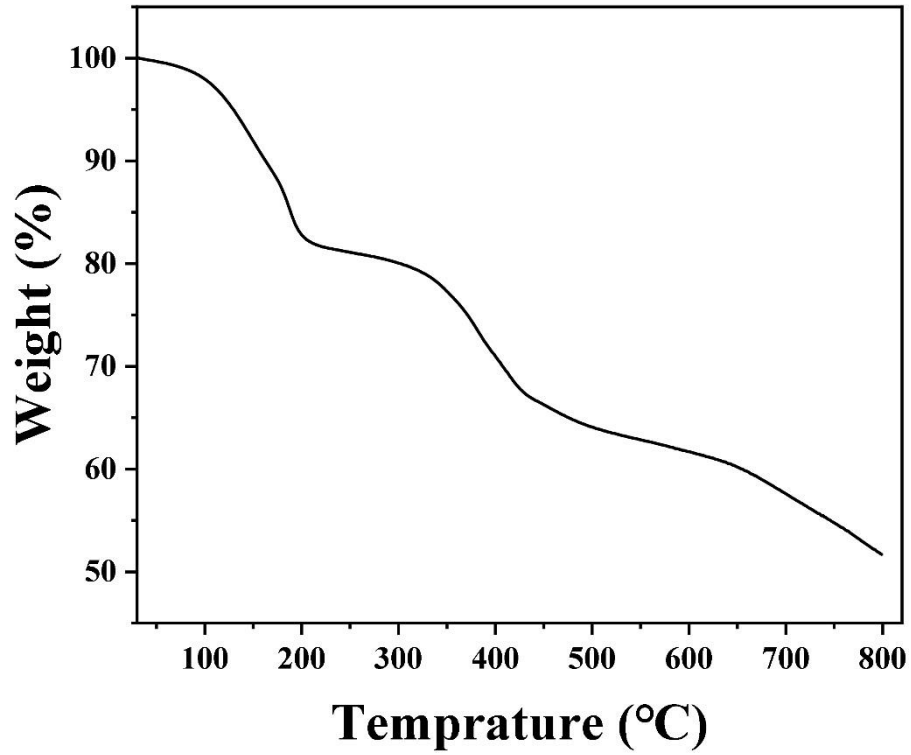

Figure S4. Thermogravimetric analysis of Mn−TCPP(Ru).

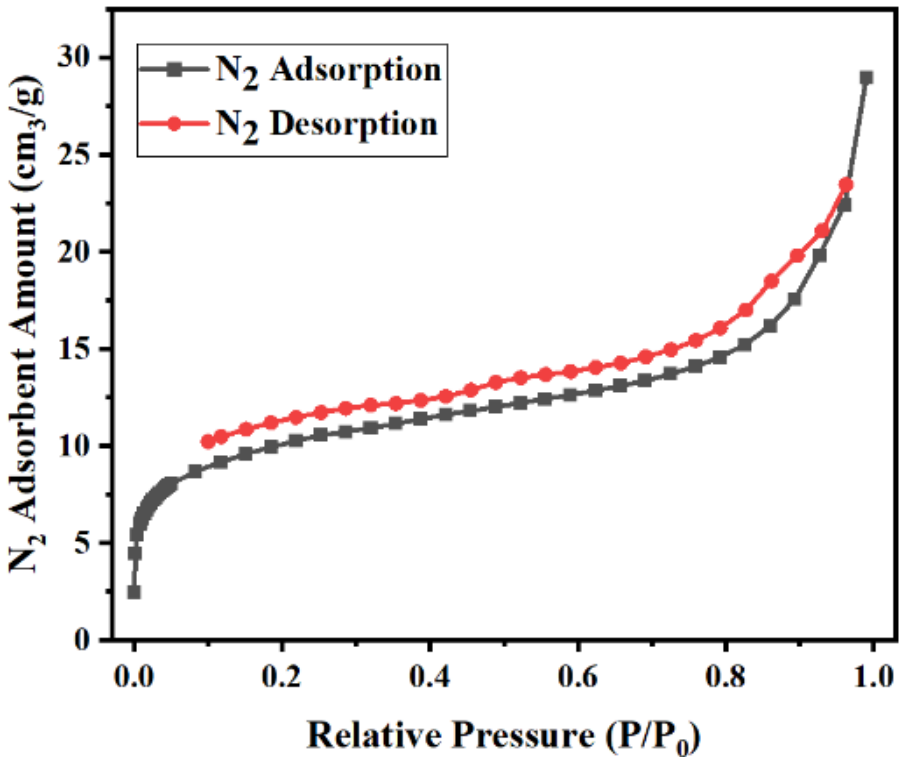

Figure S5. Nitrogen sorption isotherms for Mn−TCPP(Ru) at 77 K.

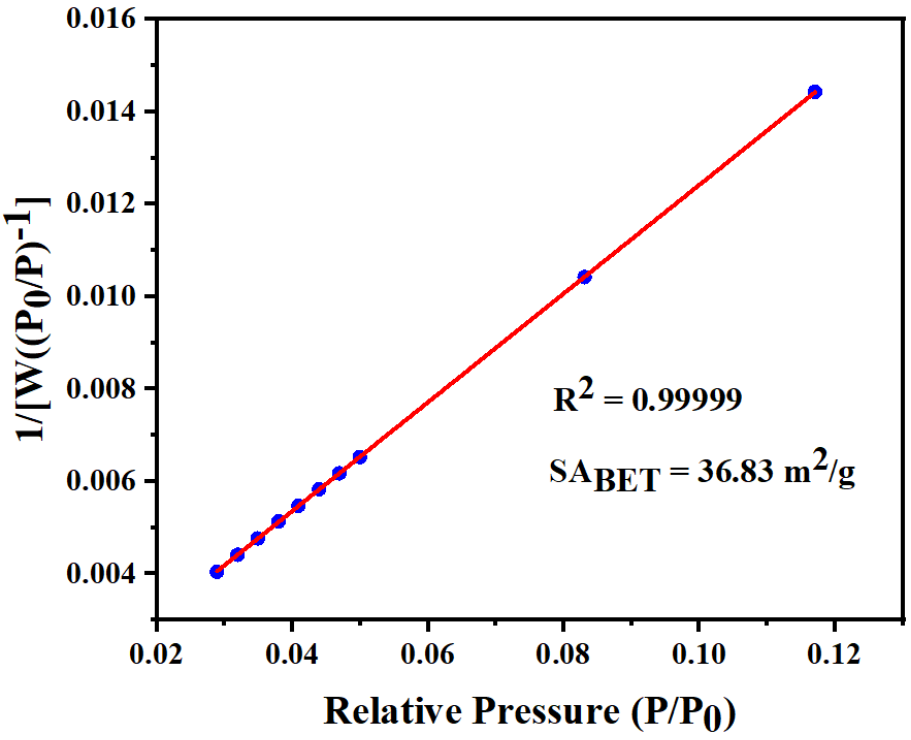

Figure S6. Plot of the linear region on the nitrogen isotherm of Mn−TCPP(Ru) for the BET equation.

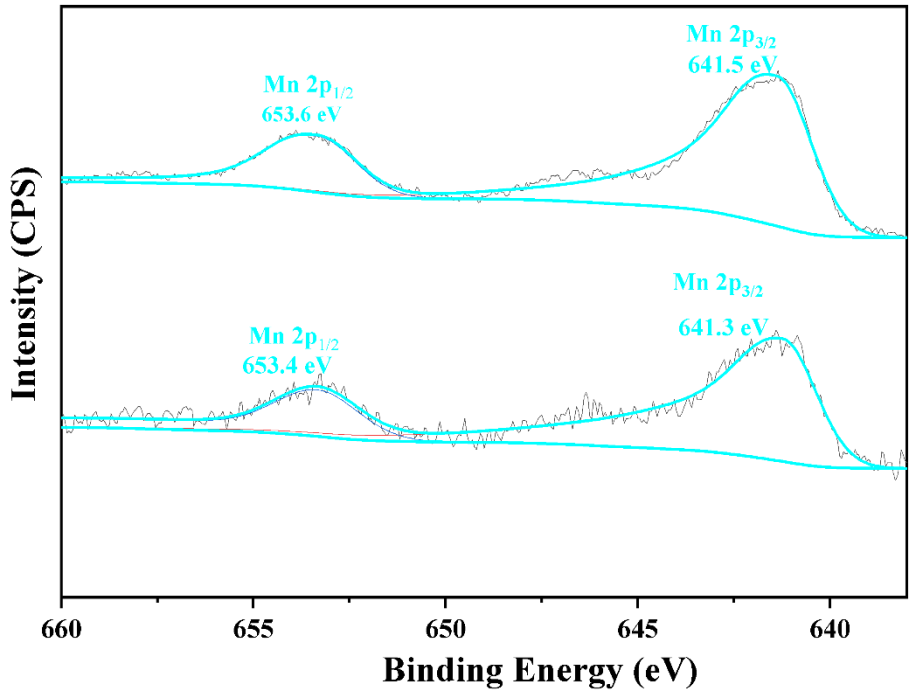

Figure S7. XPS spectra of Mn-TCPP(Ru) Mn 2p before and after the reaction.

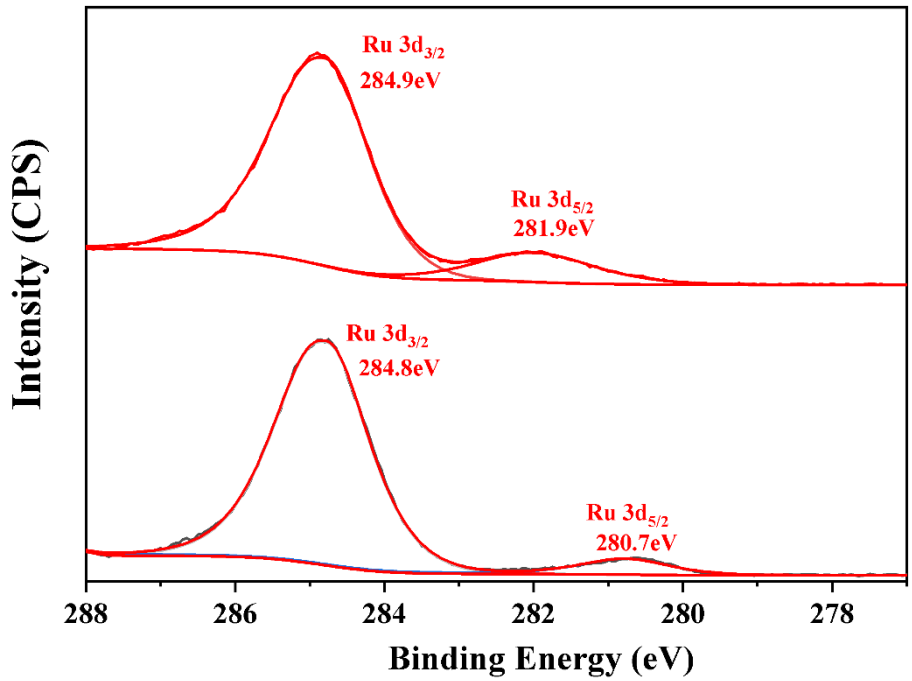

Figure S8. XPS spectra of Mn-TCPP(Ru) Ru 3d before and after the reaction.

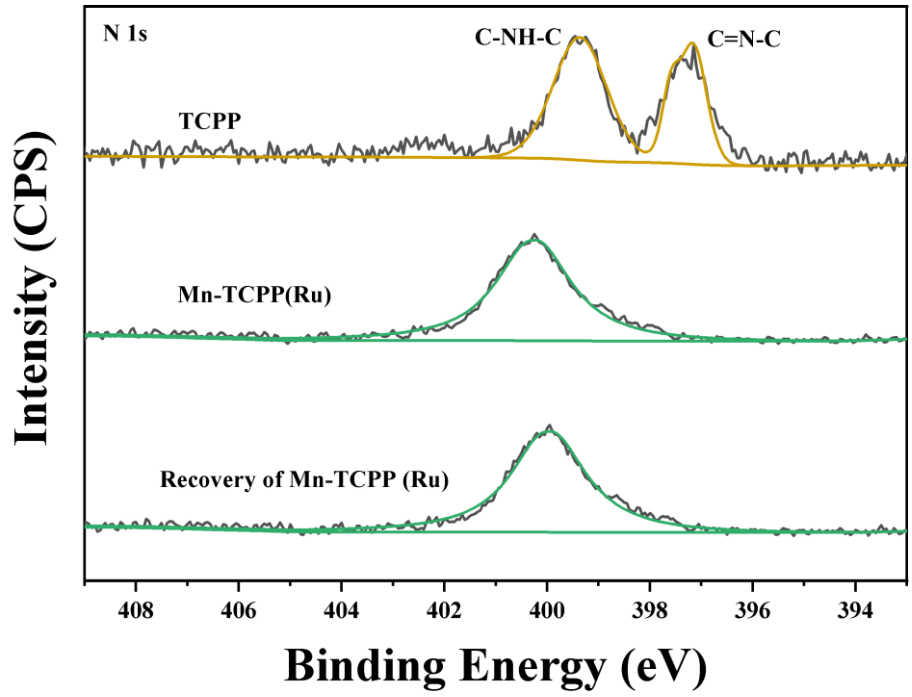

Figure S9. XPS spectra of TCPP, Mn-TCPP(Ru) before reaction, and Mn-TCPP(Ru) after reaction.

4. Catalysis Details

Typical Procedure for C (sp^3)-H Oxidation with TBHP.

In a typical reaction, the catalytic reaction was conducted in a 7 mL sealed reactor which was equipped with water bath and a temperature control system with catalyst (0.005 mmol), 70% TBHP (in water) (15 μL), substrate (13μL), and acetonitrile (2.5 mL). The vessel was stirred under 50 ℃ for 24 hours. After the reaction, the catalysts were separated by centrifugation. The residual liquid was taken to be analyzed by GC analysis to calculate the product amount of the reaction with respect to 1,3,5-trimethoxylbenzene as an internal standard.

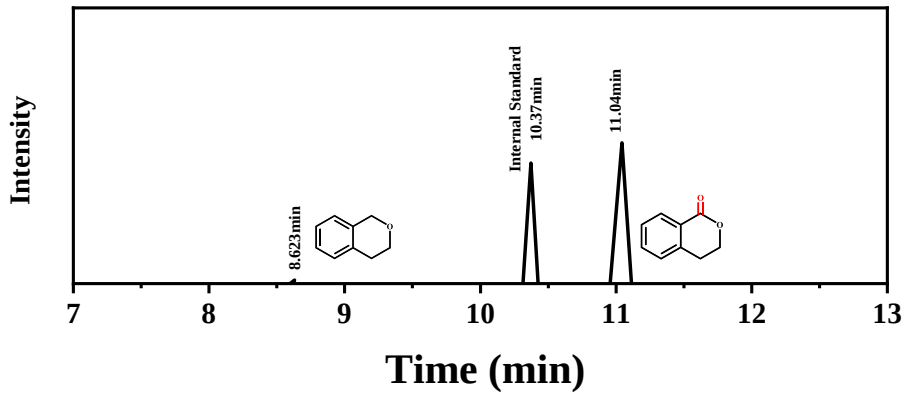

Figure S10. GC trace of the products in Isochroman oxidation with Mn−TCPP(Ru) and TBHP in oxygen atmosphere.

Table S3. C(sp^3)-H Bond Oxidation of Isochroman with Different Conditions.

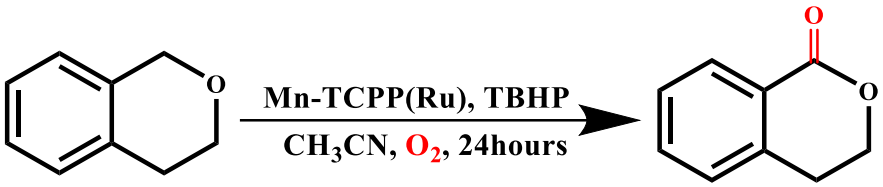

Entry	Changes	Cover (%)
1	None	92.3
2	Without Mn−TCPP(Ru)	N.R.
3	Without TBHP	trace
4	airs instead of O_2	76.5
5	Ar instead of O_2	trace
6	TCPP(Ru)	34.7
7	TCPP(H)	N.R.
8	$MnCl_2·4H_2O$	N.R.
9	TCPP(Ru)+ $MnCl_2·4H_2O$	51.8
10	DMF instead of CH_3CN	16.3
11	$C_{12}O_{12}Ru_3$	25.2
12	[Cu $(CH_3CN)_4$]BF_4	N.R.

Reaction Conditions: Catalysts (5.0 mol %), Isochroman (13μL), TBHP (15μL), CH_3CN (2.5 mL), O_2 (1 atm), 50 ℃, 24 hours. The product amounts were calculated according to the gas chromatography (GC) analysis for 1, 3, 5-trimethox-ylbenzene as an internal standard, N.R. = no reaction.

Cycle Catalysis Experiment.

After each catalysis, the catalyst Mn−TCPP(Ru) was collected by filtering, then it was washed and dried for the next experiment. The yield after running five times did not decrease obviously.

Table S4. Cycle Catalysis Experiment for C(sp^3)-H Bond Oxidation of Isochroman.

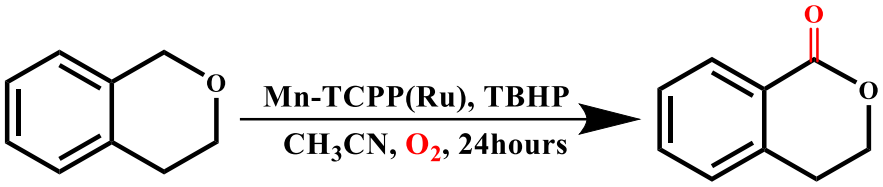

Run	Cover (%)
1	100
2	95.9
3	95.87
4	89.01
5	88.23

Table S5. Conversion tracking experiment for C(sp^3)-H bond oxidation of Isochroman at different temperatures.

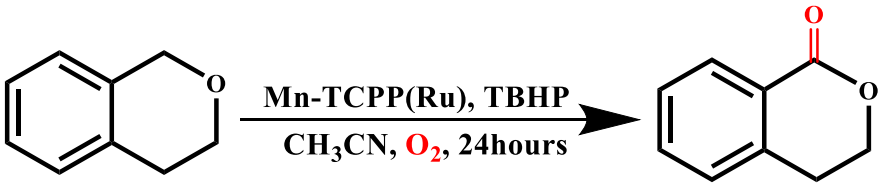

Time/hours	Products (μmol)		
	30 ℃	40 ℃	50 ℃
0	0	0	0
6	25.56	43.70	60.20
12	50.13	72.57	92.51
18	72.82	95.29	121.4
24	101.2	123.2	140.0

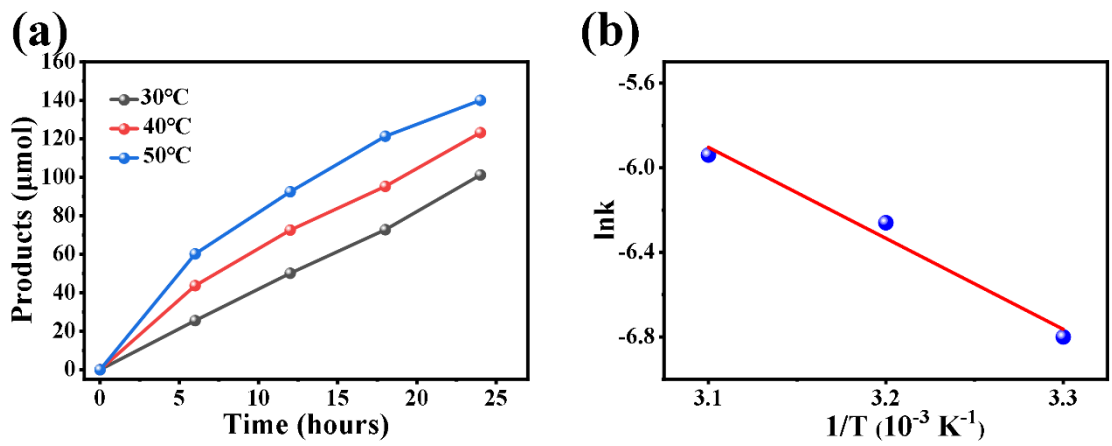

Figure S11. (a) Conversion tracking experiment for C(sp^3)-H bond oxidation of Isochroman at different temperatures; (b) The zero-order reaction kinetic model was established by using the integral rate equation from the results of kinetic reactions at different temperatures.

Table S6. Conversion tracking experiment for inert C(sp^3)-H bond oxidation of Isochroman at different concentrations of auxiliary oxidant TBHP.

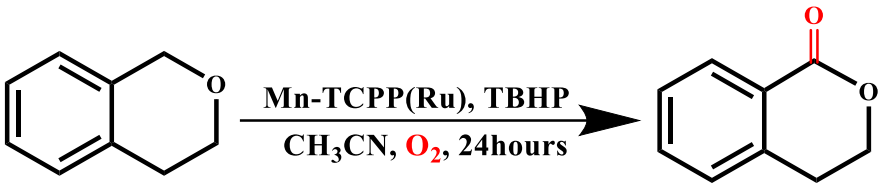

Time/hours	Products (μmol)		
	0.1 mmol TBHP	0.2 mmol TBHP	0.3 mmol TBHP
0	0	0	0
6	60.20	62.41	63.84
12	92.51	95.71	97.26
18	121.4	124.6	126.3
24	140.0	143.5	149.7

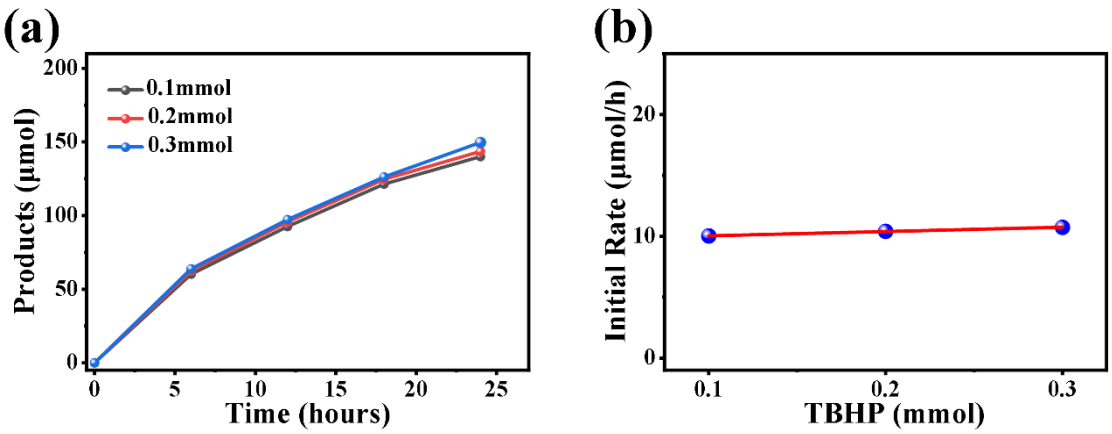

Figure S12. (a) Conversion tracking experiment for C(sp^3)-H bond oxidation of Isochroman at different concentrations of auxiliary oxidant TBHP; (b) The initial conversion rate of kinetics reactions of different TBHP concentrations.

Table S7. Conversion tracking experiment for inert C(sp^3)-H bond oxidation of Isochroman at different loading of Mn−TCPP(Ru)

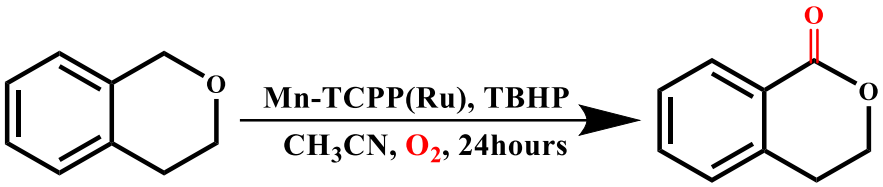

Time/hours	Products (μmol)		
	5 μmol Mn−TCPP(Ru)	10 μmol Mn−TCPP(Ru)	15 μmol Mn−TCPP(Ru)
0	0	0	0
6	60.2	62.41	63.84
12	92.51	95.71	97.26
18	121.4	124.6	126.3
24	140.0	143.5	149.7

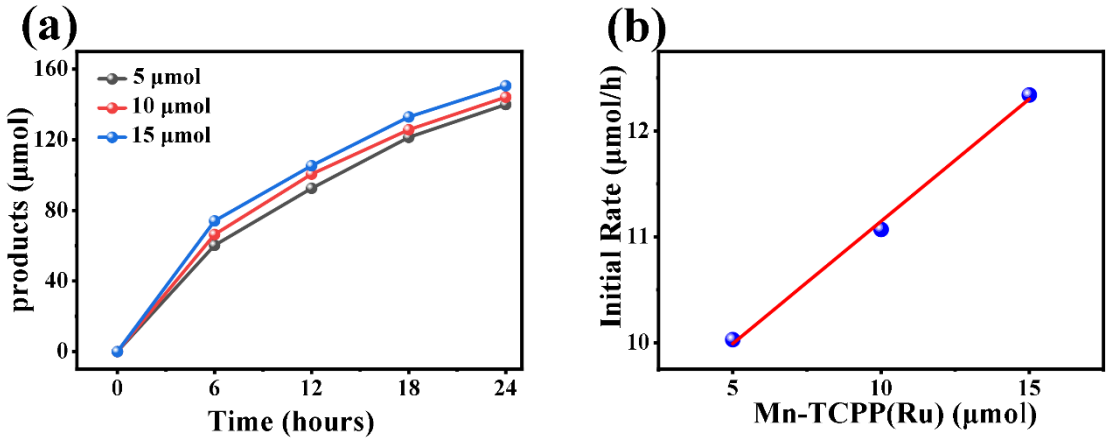

Figure S13. (a) Conversion tracking experiment for C(sp^3)-H bond oxidation of Isochroman at different loading of Mn−TCPP(Ru); (b) The initial conversion rate of kinetics reactions of different MOF loading.

EPR Spectroscopy.

According to the relative literature,[S5]Spin trapping experiments were performed according to the following general procedure: a solution of N-tertbutyl-α-phenylnitrone (PBN) (0.5 mol L^{-1}) in dry deoxygenated MeCN was prepared prior to the measurements and kept in a freezer at -20 ºC.

In *situ* experiment: A solution of PBN was mixed with a solution containing a mixture of ^{t}BuOOH and MOFs in MeCN (ratios as for the optimized oxidation procedure). The solution was sampled in a glass capillary (0.9-1.1 mm od), placed in the spectrometer equipped with a cryostat and measured immediately.

Table S8. The scope of ethers and alkanes in the C−H bonds activation[a].

Entry	Substrate	product	Conver (%)
1	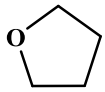	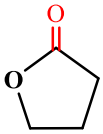	62
2	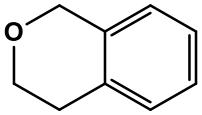	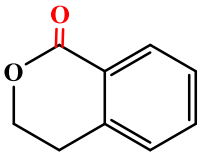	92
3	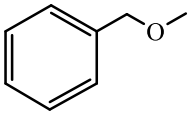	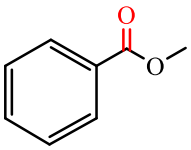	52
4	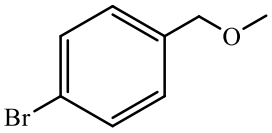	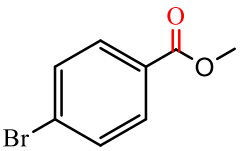	63
5	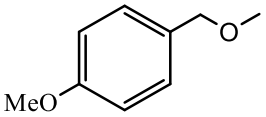	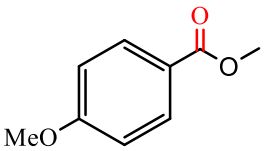	56
6	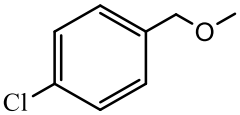	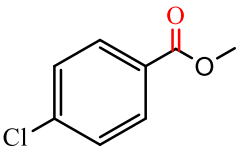	65
7	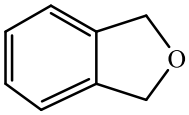	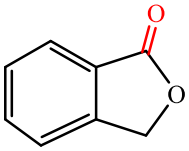	92
8	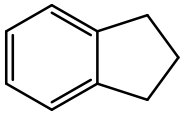	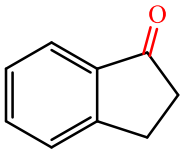	62
9	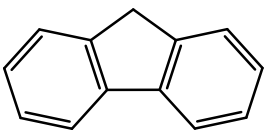	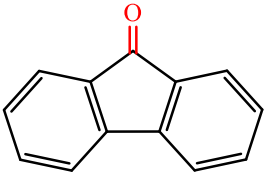	87

"Reaction conditions: Substrate (0.1mmol), TBHP (0.1 mmol), Mn−TCPP(Ru) (5 mol %) and acetonitrile (2.5 mL) in O_2 atmosphere (1 atm) at 50℃ for 24 hours. The product amounts were calculated according to the GC analysis with respect to 1, 3, 5-trimethoxylbenzene as an internal standard.

5. Gas Chromatogram.

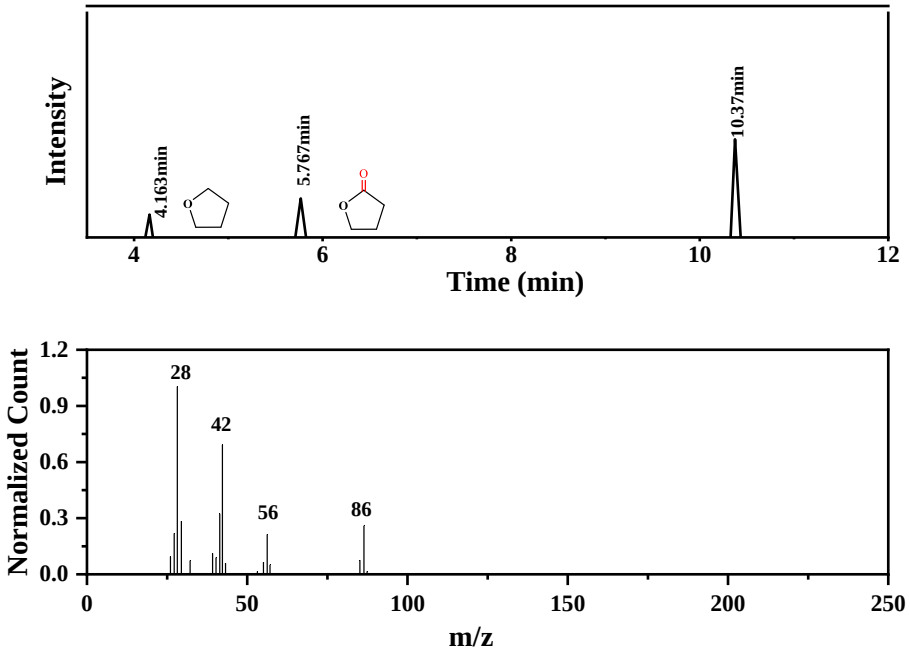

Figure S14. GC and GC-MS data of catalytic reactions of 1a.

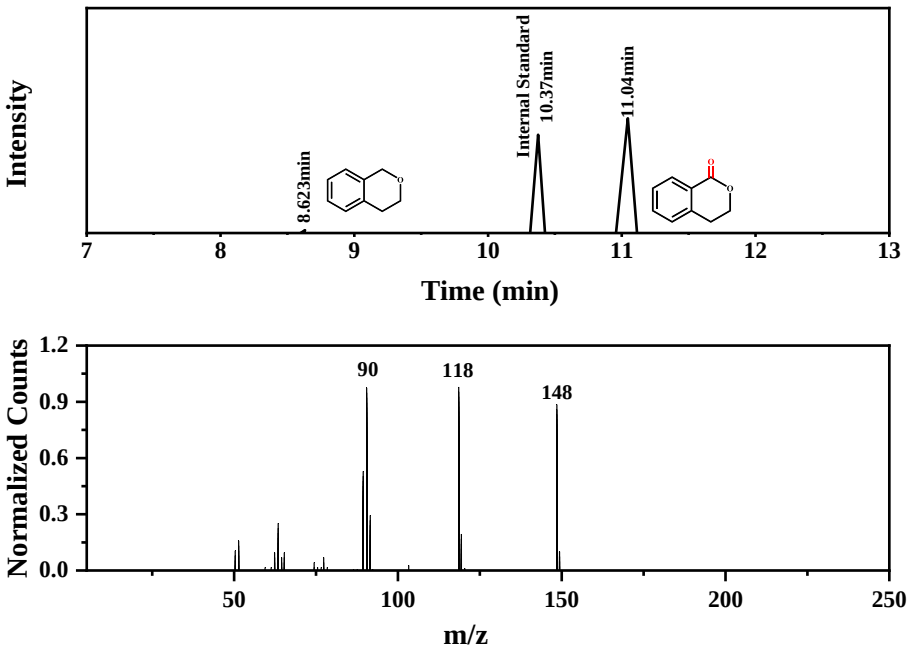

Figure S15. GC and GC-MS data of catalytic reactions of 1b.

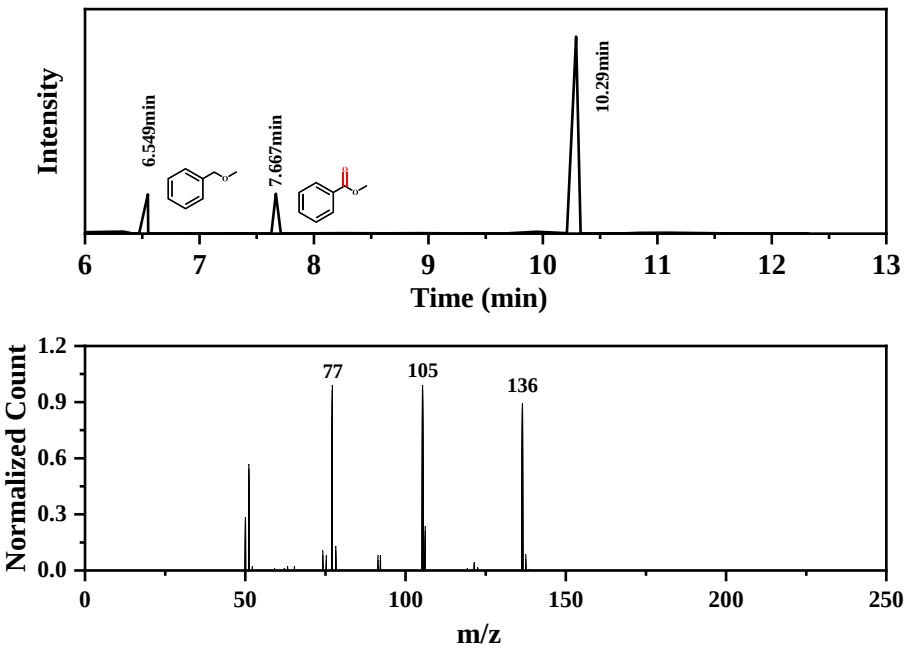

Figure S16. GC and GC-MS data of catalytic reactions of 1c.

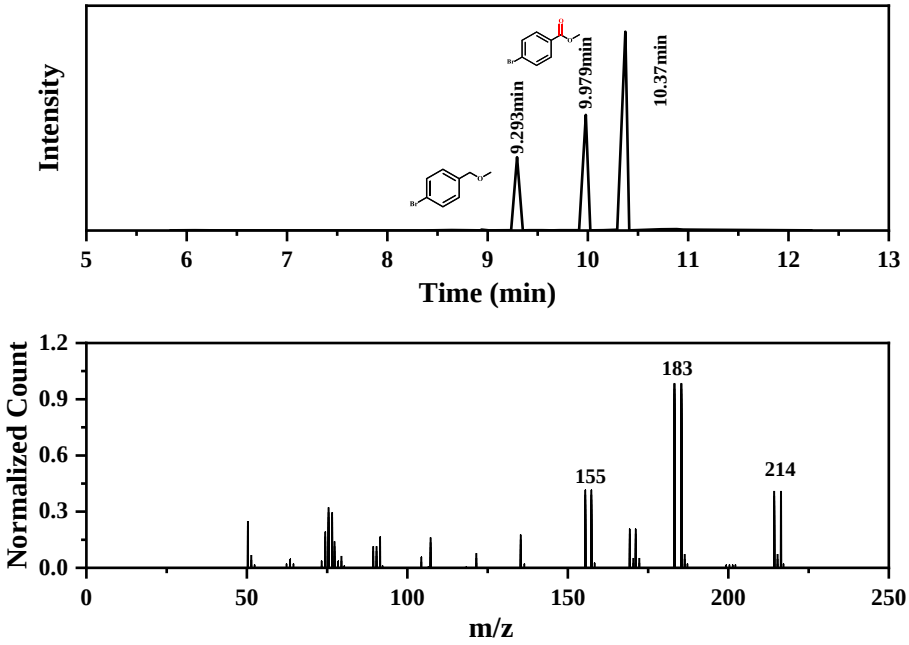

Figure S17. GC and GC-MS data of catalytic reactions of 1d.

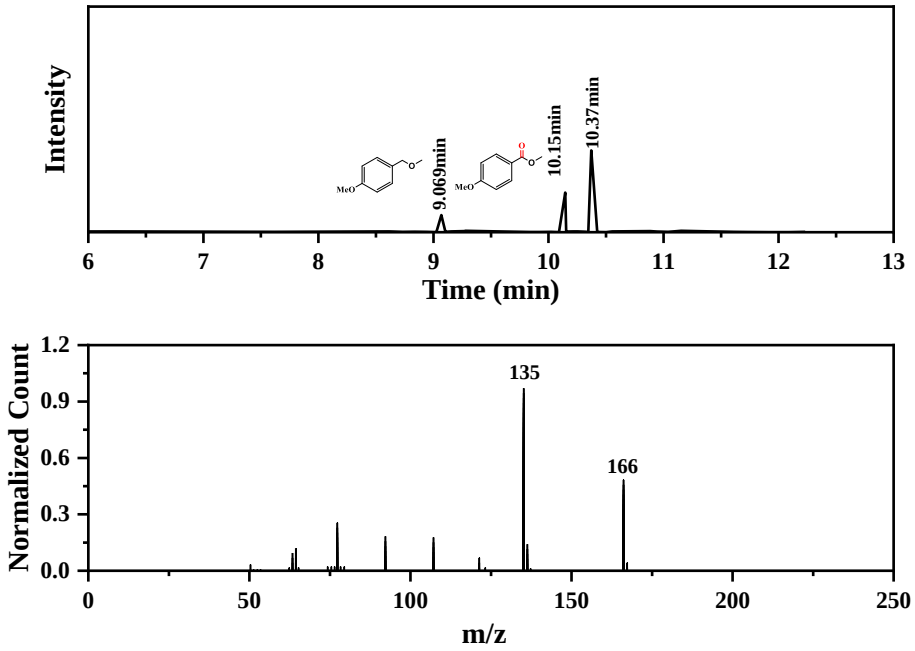

Figure S18. GC and GC-MS data of catalytic reactions of 1e.

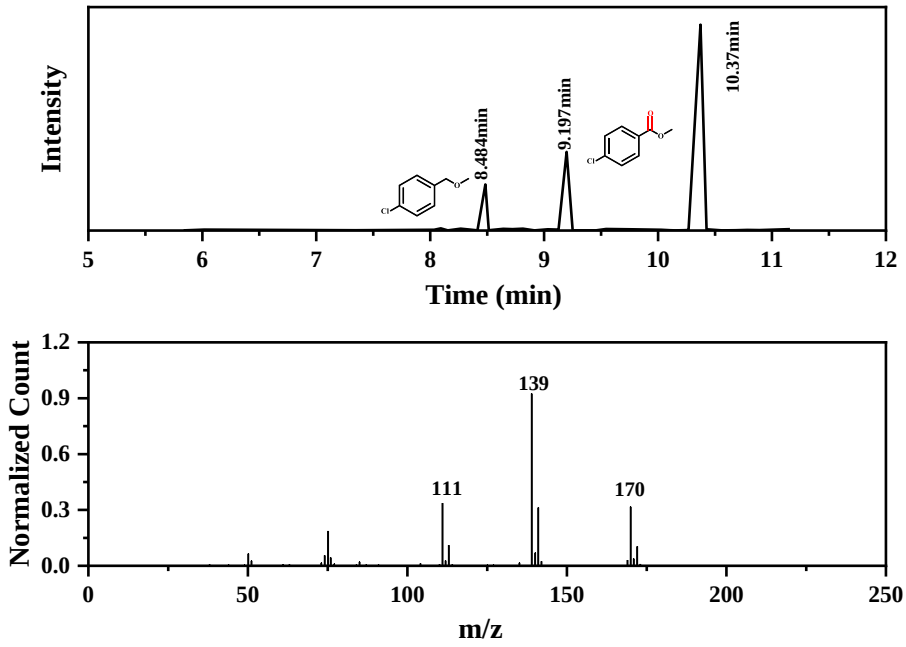

Figure S19. GC and GC-MS data of catalytic reactions of 1f.

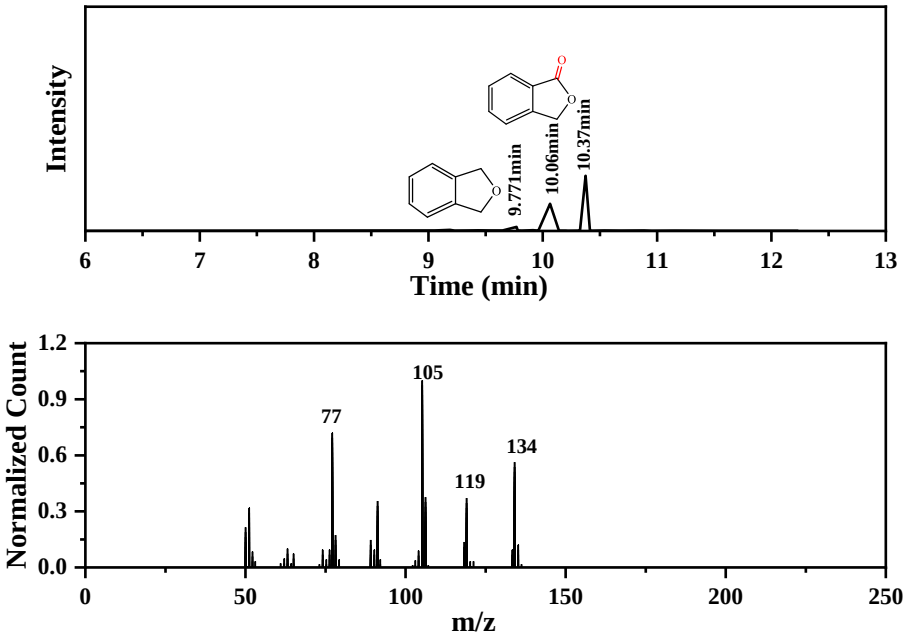

Figure S20. GC and GC-MS data of catalytic reactions of 1g.

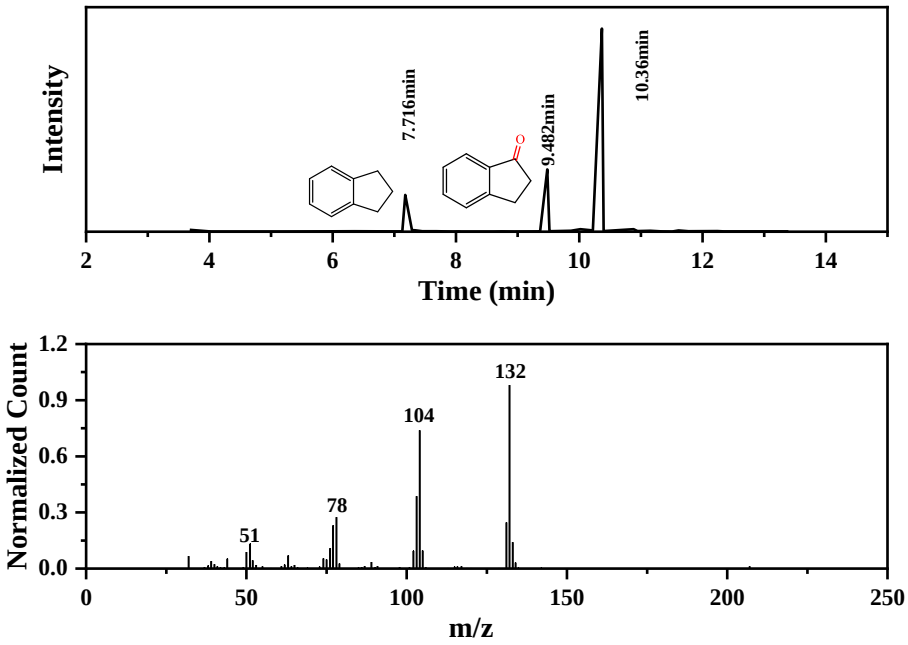

Figure S21. GC and GC-MS data of catalytic reactions of 1h.

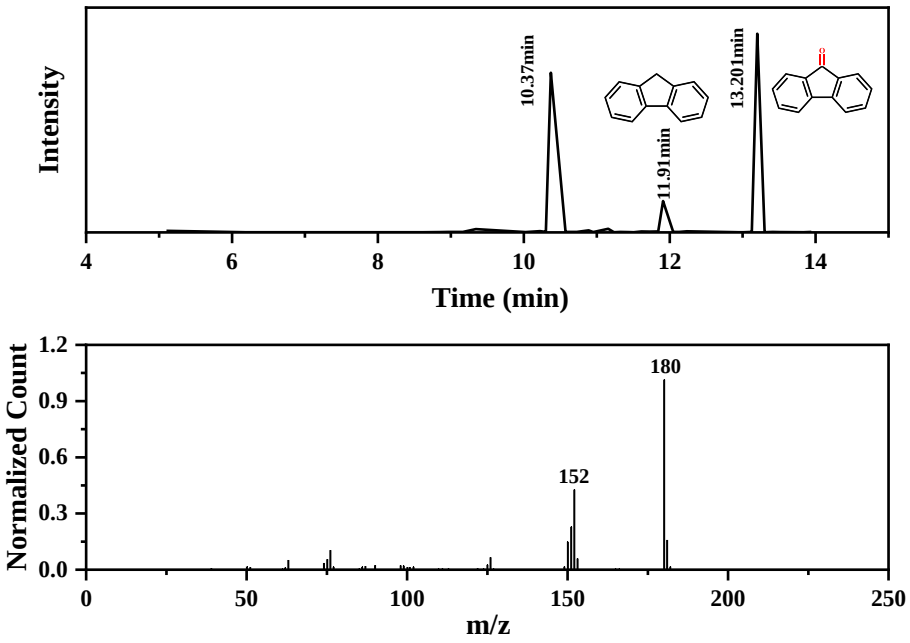

Figure S22. GC and GC-MS data of catalytic reactions of 1i.

6. ^{1}H NMR Spectra

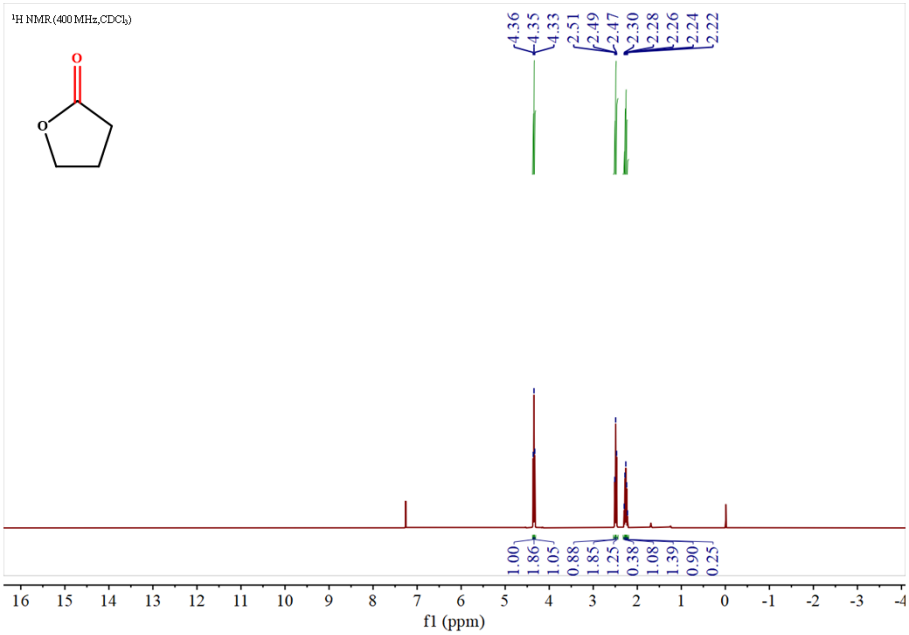

Figure S23. ^{1}H NMR spectrum of 1a.

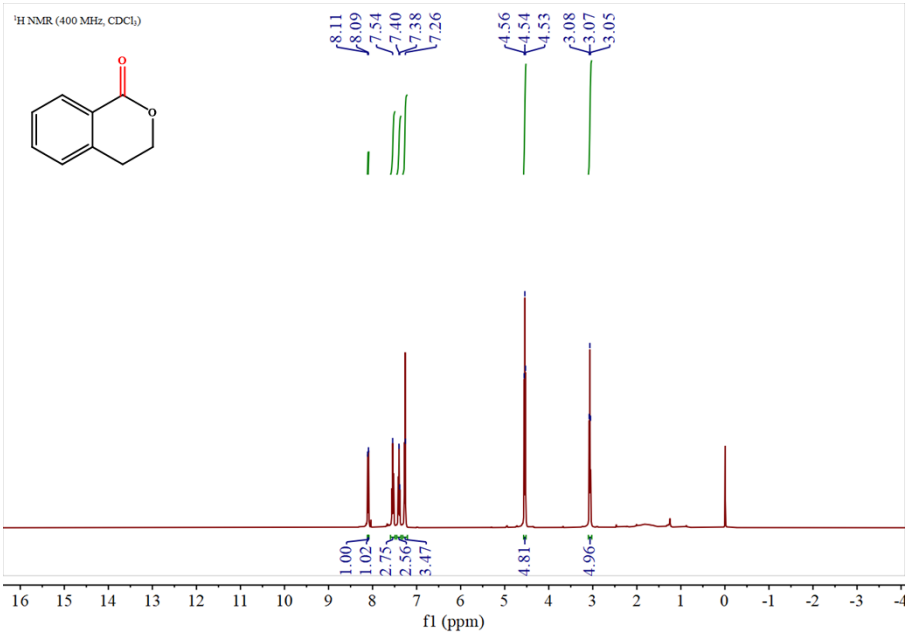

Figure S24. ^{1}H NMR spectrum of 1b.

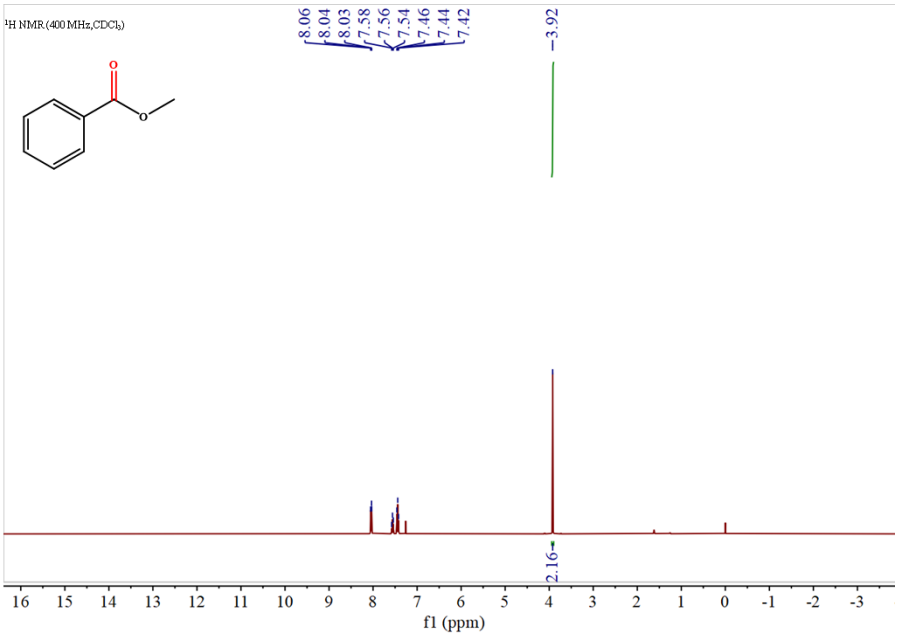

Figure S25. ^{1}H NMR spectrum of 1c.

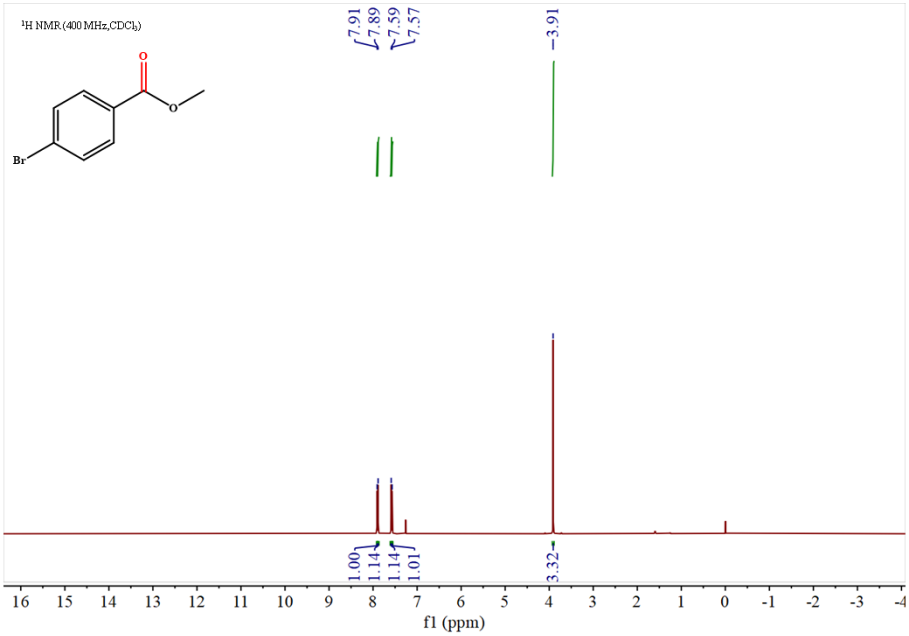

Figure S26. ^{1}H NMR spectrum of 1d.

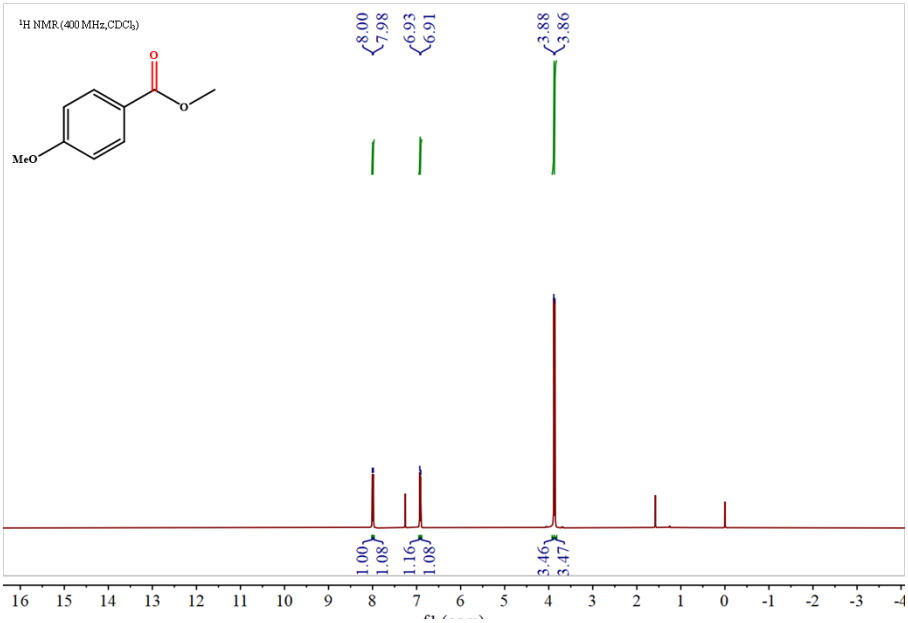

Figure S27. ^{1}H NMR spectrum of 1e.

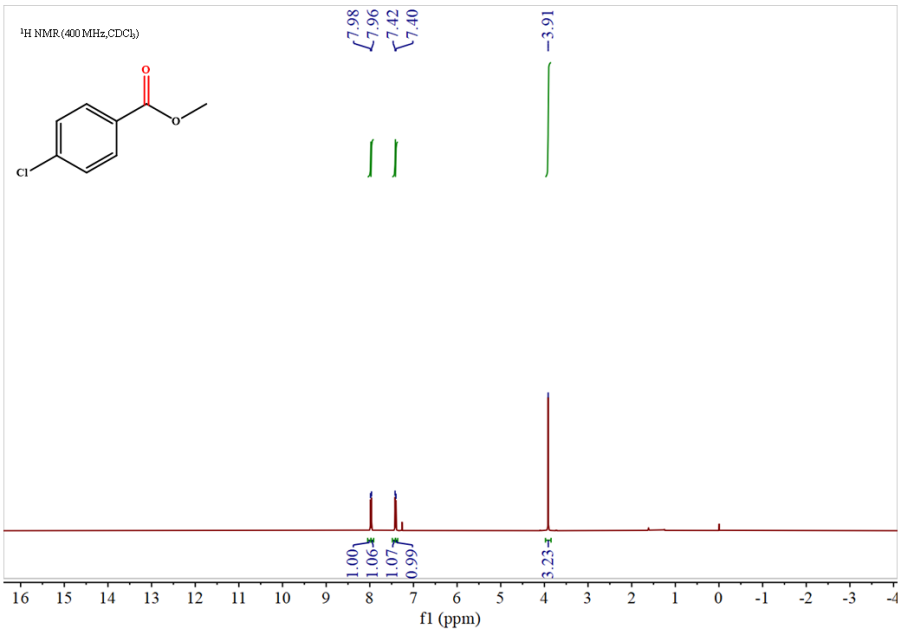

Figure S28. ^{1}H NMR spectrum of 1f.

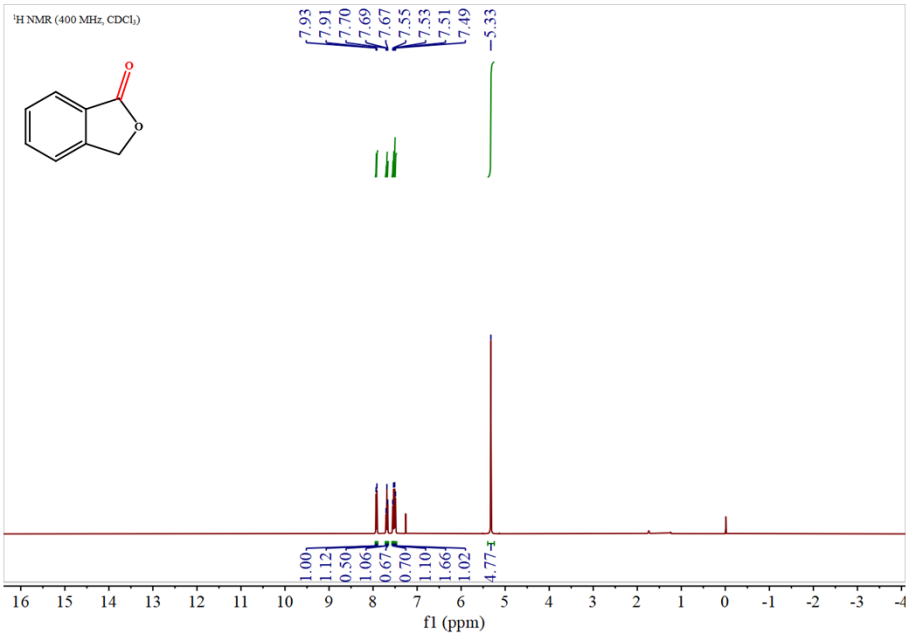

Figure S29. ^{1}H NMR spectrum of 1g.

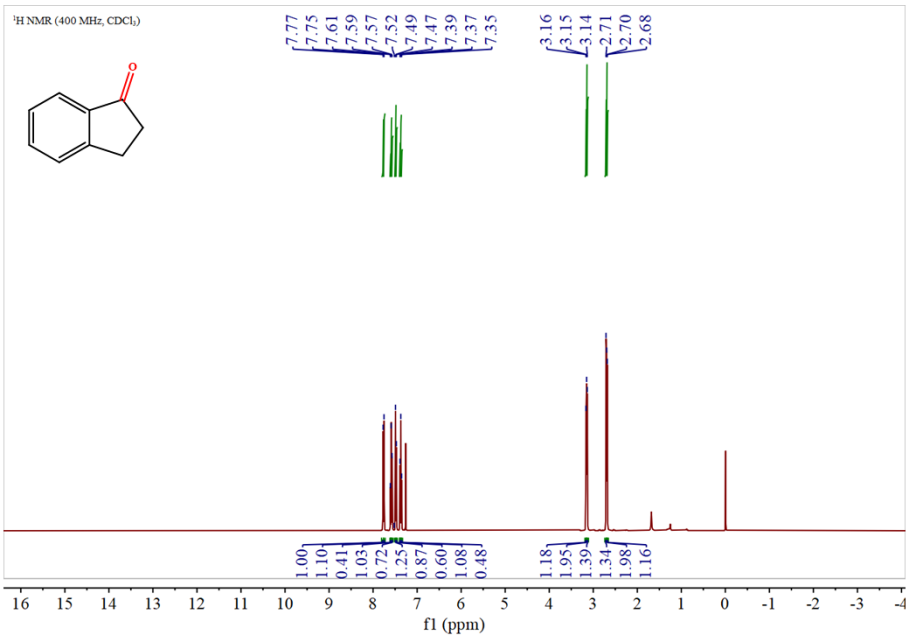

Figure S30. ^{1}H NMR spectrum of 1h.

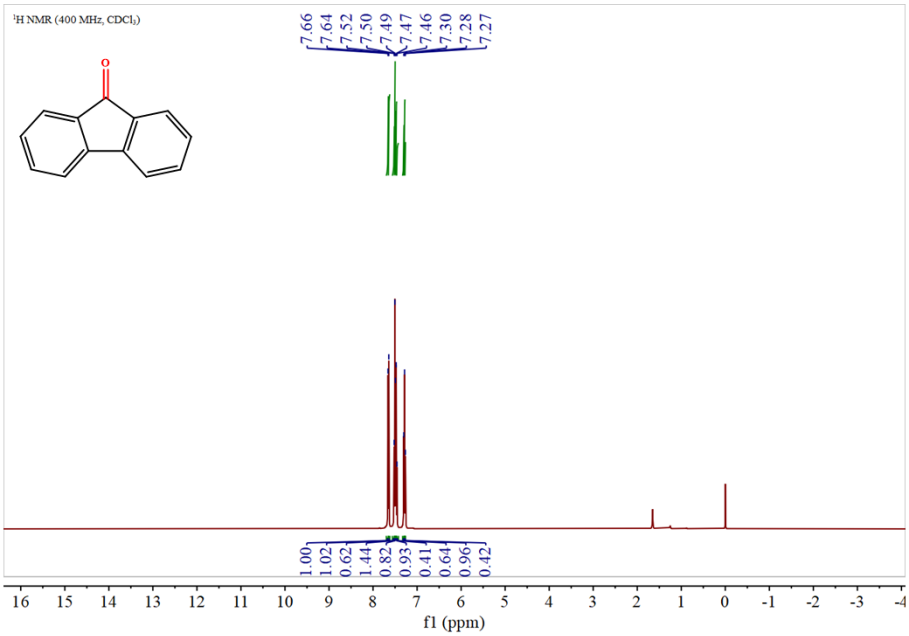

Figure S31. ^{1}H NMR spectrum of 1i.

7. References

S1. Liu, T.-F.; Feng, D.; Chen, Y.-P.; Zou, L.; Bosch, M.; Yuan, S.; Wei, Z.; Fordham, S.; Wang, K.; Zhou, H.-C., *J. Am. Chem. Soc.* 2014, **137** (1), 413-419.

S2. Chen, L.; Cui, H.; Wang, Y.; Liang, X.; Zhang, L.; Su, C.-Y., *Dalton Trans.* 2018**, 47** (11), 3940-3946.

S3. Sheldrick, G. M., *Acta Crystallogr. C Struct. Chem.* 2015, **71** (1), 3-8.

S4. Spek, A. L , *J. Appl. Crystallogr*. 2003, **36**, 7−13

S5. Kimberley, L.; Sheveleva, A. M.; Li, J.; Carter, J. H.; Kang, X.; Smith, G. L.; Han, X.; Day, S. J.; Tang, C. C.; Tuna, F.; McInnes, E. J. L.; Yang, S.; Schröder, M., *Angew.* 2021**, 60** (28), 15243-15247.